ARTICLE
Journal of Cellular Biochemistry 111:1377–1389 (2010)

Journal of Cellular Biochemistry

Flashing Light Signaling Circuit in Sponges: Endogenous Light Generation After Tissue Ablation in *Suberites domuncula*

Matthias Wiens,[1] Xiaohong Wang,[2] Andreas Unger,[3] Heinz C. Schröder,[1] Vladislav A. Grebenjuk,[1] Dario Pisignano,[4] Klaus P. Jochum,[5] and Werner E.G. Müller[1*]

[1]*Institute for Physiological Chemistry, Johannes Gutenberg University, Medical School, Duesbergweg 6, D-55099 Mainz, Germany*

[2]*National Research Center for Geoanalysis, Chinese Academy of Geological Sciences, 26 Baiwanzhuang Dajie, CHN-100037 Beijing, China*

[3]*Max Planck Institute for Polymer Research, Postfach 3148, D-55128 Mainz, Germany*

[4]*Scuola Superiore ISUFI, Università del Salento, and National Nanotechnology Laboratory, Istituto Nazionale di Fisica della Materia-Consiglio Nazionale Delle Ricerche, I-73100 Lecce, Italy*

[5]*Max Planck Institute for Chemistry, Postfach 3060, D-55020 Mainz, Germany*

ABSTRACT

The skeleton of siliceous sponges (phylum Porifera: classes Demospongiae and Hexactinellida), composed of tightly interacting spicules that assemble to a genetically fixed scaffold, is formed of *bio-silica*. This inorganic framework with the quality of quartz glass has been shown to operate as light waveguide in vitro and very likely has a similar function in vivo. Furthermore, the molecular toolkit for endogenous light generation (luciferase) and light/photon harvesting (cryptochrome) has been identified in the demosponge *Suberites domuncula*. These three components of a light signaling system, spicules–luciferase–cryptochrome, are concentrated in the surface layers (cortex) of the poriferan body. Specimens from which this cortex has been removed/ablated do not emit light. However, with regeneration and reconstitution of the cortex the animals re-gain the capacity to flash light. This newly discovered characteristic of sponges to generate light prompted us to investigate the genetic basis for the endogenous light signaling system. As a potential transcription factor involved in the expression of luciferase and cryptochrome, a SOX-related protein has been identified. In dark-adapted animals or in tissue from below the cortex region, the medulla, no gene or protein expression of SOX-related protein, luciferase, and cryptochrome could be detected. However, during the regeneration of the cortex, a stage-specific expression pattern was recorded: SOX-related protein > luciferase > cryptochrome. We conclude that a flashing light signaling circuit exists, which might control the retinoic acid-induced differentiation of stem cells into pulsating and contracting sponge cells, that is, pinacocytes and myocytes. J. Cell. Biochem. 111: 1377–1389, 2010.

KEY WORDS: SPONGES; PORIFERA; *SUBERITES DOMUNCULA*; LIGHT EMISSION; LIGHT SIGNALING CIRCUIT; SOX-RELATED PROTEIN; LUCIFERASE; CRYPTOCHROME

In contrast to most other animal phyla, which possess calcium carbonate or phosphate-based skeletal elements, two classes of sponges (Demospongiae and Hexactinellida) produce a bio-siliceous skeleton [Lowenstam and Weiner, 1989]. The third class of Porifera that emerged later in evolution, the Calcarea, has a calcareous skeleton [see Wang et al., 2010]. The earliest well-preserved sponge species with a hard skeleton were hexactinellids from the Niutitang Formation (Sancha; China) [Steiner et al., 1993]. In general, the inorganic skeleton of Metazoa must fulfill three prerequisites: (i) support the organic tissue, (ii) protect against physical and organic

Grant sponsor: German Bundesministerium für Bildung und Forschung (Project "Center of Excellence *BIOTEC*-marin"); Grant sponsor: International Human Frontier Science Program; Grant sponsor: Ministry of Science and Technology of China; the International S & T Cooperation Program of China; Grant number: 2008DFA00980; Grant sponsor: European Commission; Grant number: MRTN-CT-2004-512301, BIOCAPITAL; Grant sponsor: Deutsche Forschungsgemeinschaft; Grant number: WI 2116/2-2.

*Correspondence to: Prof. Dr. Werner E.G. Müller, Institute for Physiological Chemistry, Johannes Gutenberg University, Medical School, Duesbergweg 6, D-55099 Mainz; Germany. E-mail: wmueller@uni-mainz.de

Received 25 May 2010; Accepted 24 August 2010 • DOI 10.1002/jcb.22866 • © 2010 Wiley-Liss, Inc.
Published online 9 September 2010 in Wiley Online Library (wileyonlinelibrary.com).

stress, and (iii) facilitate motility. Obviously, the poriferan siliceous skeleton complies with two of these requirements, and both have been considered fundamental for the survival of sponges during adverse climatic situations, such as global ice periods [Wang et al., 2010]. However, it remained enigmatic whether the sponge skeleton also plays a role in migration/motility, in particular because most sponge larvae display a mobile behavior, and respond to external stimuli [see Maldonado, 2006], while almost all adult sponge species are sessile [Renard et al., 2009]. However, there is strong evidence that the evolutionary oldest poriferan species were quite mobile in their adulthood, with only a loose attachment to the seafloor [Wang et al., 2010]. In addition, despite the absence of a conventional nervous system based on neuronal cells [Pavans de Ceccatty, 1989], all sponges are provided with the intrinsic ability to contract. These contractions are vital and support the circulation of water through the poriferan aquiferous system [reviewed in Renard et al., 2009]. A few sponge species even use rhythmic body contractions for movement, for example, the demosponge *Tethya wilhelma* [Nickel, 2006].

It is amazing that during the long evolutionary history of sponges their skeletal elements, the siliceous spicules, which are composed of quartz glass [Müller et al., 2008], retained the distinguished property to operate as light waveguides [Aizenberg et al., 2004; Wang et al., 2010]. Those light guiding properties have been studied recently in several hexactinellids and demosponges [Cattaneo-Vietti et al., 1996; Müller et al., 2006; Müller et al., 2009]. From these findings it has been proposed that light that has been generated in vivo might be transmitted through the spicules and subsequently converted into electric signals via photoelectric reactions [Müller et al., 2006]. Also the complex and highly organized architecture of the skeletal system speaks for such a function [Ridley and Dendy, 1887]. It is well-known that most marine organisms which live in greater depths produce light, either intrinsically through host-encoded luciferases (monooxygenases) and luminescent proteins (e.g., *Renilla reniformis* green fluorescent protein, *Aequorea victoria* aequorin, *Anemonia sulcata* KFP1), or through luciferases encoded by symbiotic microorganisms (e.g., *Vibrio fischeri* luciferase or *Photobacterium phosphoreum* luciferase) [reviewed in Harvey, 1921; Liu et al., 2003]. Even though the presence of luciferin in sponge crude extracts had been demonstrated in the past [Shimomura, 1980], the molecular building blocks for a functional poriferan light-generating system, the luciferase/luciferin-regenerating enzymatic system of *Suberites domuncula*, have only recently been described [Müller et al., 2009]. Prior to that finding, it could be shown experimentally that electric impulses are transmitted in tissue of the hexactinellid *Rhabdocalyptus dawsoni* over distances of more than 10 mm [Leys and Mackie, 1997]. Moreover, the phenomenon of phototaxis has been extensively studied in larvae of demosponges, for example, *Amphimedon queenslandica* [Leys et al., 2002]. The property to control the phototactic reaction has been attributed to pigmented ciliated cells, forming a ring at the posterior pole of the larvae. Also other sponge larvae that are not provided with pigmented cells react to light [Elliott and Leys, 2007]. Formation of endogenous light after tactile stimulation had already been shown as early as 1921 [Harvey, 1921] in the demosponge *Grantia* sp.; however, this observation lent substance to the hypothesis that symbiotic bacteria were responsible for light generation [Aizenberg et al., 2004]. Now the identification of the *S. domuncula* luciferase indicates a sponge endogenous bioluminescence-producing system independent of any symbionts. The bioluminescence emission spectrum of the *S. domuncula* luciferase was determined to range from 470 to 640 nm [Müller et al., 2009]. Hence, this spectrum overlaps with the light transmission spectrum found to be characteristic for the sponge spicules [Müller et al., 2006], which ranges from 620 to 1,250 nm (red/orange wavelength components of the visible light).

Furthermore, the discovery of cryptochrome(s), which are crucially involved in light harvesting reactions in corals [Levy et al., 2007] stimulated a systematic screening for homologous poriferan proteins, resulting in the identification of candidate molecules in demosponges (*S. domuncula*) as well as in hexactinellids (*Crateromorpha meyeri*) [Müller et al., 2010]. As in the coral model [Levy et al., 2007], the expression of poriferan cryptochrome is controlled by light [Müller et al., 2010]. More specifically, the expression of the *S. domuncula* cryptochrome gene after light exposure (light source within this range also 330–900 and 700–1,100 nm [Müller et al., 2010]) is primarily restricted to the surface zone of the animal, suggesting that the photo-activated protein is compartmentalized in the *cortex* (the outer tissue layer). Similarly, the expression of poriferan luciferase is light-adapted [Müller et al., 2009]. These findings prompted us to search for *upstream localized* transcription factors (TF) controlling the expression of cryptochrome and luciferase, the key molecules that are involved in the proposed photoreception/photogeneration system in sponges. A poriferan homolog of Pax-6, a molecule that is required for morphogenesis of the visual system in triploblasts [Gehring and Ikeo, 2009] could not be detected. Therefore, we screened for SOX genes, encoding a family of metazoan-specific TF [Koopman et al., 2004] that have been found to play important roles in a variety of developmental processes, particularly during organogenesis [Wegner, 1999]. All SOX proteins comprise a highly conserved high mobility group (HMG) box. Among the over 30 family members known so far, in particular one protein, SOX-2 [Hagstrom et al., 2005], has been implicated in the early human eye and brain development.

In the present study, we analyzed the spatio-temporal expression of *S. domuncula* genes, coding for a *SOX-related protein*, a *luciferase*, and a *cryptochrome*, following ablation of the surface cell layers. Shortly after the expression of the potential photosensory proteins (ca. 10 h) the specimens emitted light. With this study we provide for the first time data that demonstrate the existence of a genetically controlled light signaling circuit in sponges.

MATERIALS AND METHODS

CHEMICALS, MATERIALS, AND ENZYMES

The sources of most chemicals and reagents used here have been given earlier [Müller et al., 2009]; others were obtained from Sigma–Aldrich (Taufkirchen, Germany). In addition, Nutrimarine (containing glucose, biotin, folic acid, niacin, pantothenic acid, vitamin B complex) has been purchased from GroTech Aquarientechnik (Affalterbach, Germany) and Coral Trace (calcium, bicarbonate, trace elements) from Red Sea Fish Pharm (Eilat, Israel).

SPONGES

Specimens of the marine sponge *S. domuncula* (Porifera, Demospongiae, Hadromerida, Suberitidae) were collected in the Northern Adriatic near Rovinj (Croatia) from depths of 20–30 m. They were kept in Mainz (Germany) in aquaria at a temperature of 17°C for more than 5 months; where indicated the specimens were exposed to light (a 25 m^2 kg/s^3 light bulb) [Schröder et al., 2002]. During cultivation the specimens were healthy, as checked by their capacity to regenerate ablated tissue or their potential to produce asexual reproduction bodies, the gemmules [Müller et al., 2002]. While most sponge specimens harbor a hermit crab, *Pagurites oculatus* (Decapoda: Paguridea), which resides predominantly in shells of the mollusk *Trunculariopsis trunculus* (Gastropoda: Muricidae), some are devoid of crabs [see Schröder et al., 2002]. Such specimens were used for the light emitting studies; prior to the experiments they were adapted to a temperature of 22°C for 2 weeks to avoid heat stress. The animals were fed every second day with 0.5 ml of NutriMarine and 0.1 ml of Coral Trace per 20 L of seawater.

In one series of experiments tissue slices were obtained from dark-adapted specimens (kept for more than 2 weeks in the absence of light). Then the animals were exposed to red light from a distance of 6–5 cm by using an optical filter OG590 (Schott–AdvancedOptics, Mainz, Germany) in front of a white light bulb [50 m^2 kg/s^3 (General Electric, Fairfield, CT) 29208 projector white light bulb]. The OG590 filter cuts off light <500 nm and allows a maximal transmission of light >650 nm. In parallel the tissue slices were exposed to green light with the filter VG9 (Schott; cut off below 400 nm; maximum at 520 nm) and finally with blue light by using a N-WG320 filter (Schott; cut off below 300 nm; maximum at >400 nm). The intensity of the light was adjusted to 10 lux. After an exposure time for up to 24 h RNA was extracted and subjected to Northern blot analysis.

LIGHT RECORDING DEVICE

A sponge specimen was placed in a 1.0 L beaker under optimal conditions [Schröder et al., 2002]. Prior to the experiments, the specimen remained for 3 days in complete darkness in a vibration-free cabinet (22°C). Then, a 2–3 mm thick tissue slice was ablated from the surface (cortex) during a 30 s period of illumination (a 5 m^2 kg/s^3 light bulb). Specimens, were then fixed with a forceps under very slight pressure to the glass wall. Subsequently, the animals remained again for 3 days in complete darkness. A photomultiplier (Type H7421; Hamamatsu, Herrsching, Germany), consisting of a photocathode to detect photons from 300 to 890 nm wavelength was coupled to the 1.5 mm thick glass beaker (Fig. 2B). Data were acquired at a time resolution of 0.1 s with an HP 53131A Universal Counter (Agilent Technologies, Palo Alto, CA) and subsequently recorded through a customized script on a PC with an *IEEE-488 interface card* (Keithley, Cleveland, OH). The script allowed readout of the number of recorded counts via an IEEE-488 interface and storage of the results together with a time mark of the PC in an ASCII file. Signals were documented throughout the complete observation time.

MOLECULAR CLONING OF *S. DOMUNCULA* SOX

A fragment of a SOX-like transcript was retrieved from the *S. domuncula* EST-database (accession no. d002_003a_h09; https://octavia.vk.medizin.uni-mainz.de/login.cgi) via homology searches. The sequence, which comprises 835 nucleotides (nts), contained an open reading frame (ORF) between nt_{224} and $nt_{1,061}$ of the final sequence. The technique of polymerase chain reaction (PCR) was applied to amplify the complete cDNA, termed *SDSOX*. Thus, two insert-specific reverse primers were designed close to the *SDSOX* fragment's 5'-end (SD_SOX_R1: 5'-CTCAGCTCGGAGTTGTGCAT-3', and SD_SOX_R2: 5'-TCTTGAGCAAGCTCCTTTCTG-3') and "nested" PCR reactions were performed in combination with standard vector-specific forward primers, in order to complete the sequence. PCR conditions used were as follows: 95°C for 3 min, followed by 35 amplification cycles at 95°C for 30 s, 60°C for 30 s, 72°C for 45 s, and a final extension step at 72°C for 7 min. PCR fragments were isolated, cloned into the *pCR2.1-TOPO* vector (Invitrogen, Karlsruhe, Germany), and then used to transform *E. coli* TOP10 cells (Invitrogen). Sequencing was performed with primers directed to the vector's SP6 and T7 promoters. The complete clone (*SDSOX*), encoding the putative protein SOX_SUBDO, has a size of 1,061 nts.

SEQUENCE ANALYSES

Sequences were analyzed with computer programs BLAST (http://blast.ncbi.nlm.nih.gov/Blast.cgi) and FASTA (http://www.ebi.ac.uk/fasta33/). Multiple alignments were performed with CLUSTAL W Ver. 1.6 [Thompson et al., 1994]. The degree of support for internal branches was further assessed by bootstrapping [Felsenstein, 1993].

PREPARATION OF RECOMBINANT *S. DOMUNCULA* SOX

The complete ORF of *SDSOX* (from nt_{180} to $nt_{1,061}$, excluding M_{start} and stop codon) was amplified by touchdown PCR, using a combination of forward primer (5'-ACGATAATGTCCCGTTCGC-3') and reverse primer (5'-ATCAGATGTTGGCAAAGGAG-3'). For amplification, the following conditions were chosen, initial denaturation at 95°C for 3 min, followed by 35 amplification cycles at 95°C for 30 s, 56°C for 35 s, 72°C for 45 s, with a decreasing annealing temperature of 0.1°C in every cycle, and a final extension step at 72°C for 7 min. The resulting amplicon was TA ligated into the expression vector *pTrcHis2-TOPO* (Invitrogen), in frame with an N-terminal M_{start} and a C-terminal 6xHis-tag. Following transformation, protein expression was stimulated in BL21 cells with 1 mM isopropyl 1-thio-D-galactopyranoside (IPTG; Sigma) for 12 h. The bacterial pellet was then lysed in "BugBuster Protein Extraction Reagent" (Novagen) with 1 μl/ml of benzonase (Novagen/Merck KGaA, Darmstadt, Germany) and sonicated on ice. The cell pellet was obtained by centrifugation and, then, solubilized with lysis buffer [50 mM KH_2PO_4 (pH 8.0), 6 M urea, 300 mM KCl, 5 mM imidazole]. After centrifugation, the soluble protein was purified by affinity chromatography on Ni-IDA columns, according to the instructions of the manufacturer (Protino Ni-IDA Packed Columns; Macherey-Nagel, Düren, Germany). Purity was over 95% and checked by sodium dodecyl sulfate–polyacrylamide gel electrophoresis (SDS–PAGE). The recombinant protein was termed rSOX_SUBDO, and its

size was calculated to be 35,264 Da (including His-tag and other vector-encoded amino acid residues).

PREPARATION OF ANTIBODIES

Polyclonal antibodies (PoAb) were raised against recombinant SOX-like protein, rSOX_SUBDO, in female rabbits (White New Zealand) as described [Müller et al., 2005]. For the four injections, 10 μg each of recombinant protein [in 500 μl of phosphate-buffered saline (PBS)] were used and supplemented with 500 μl of Freud's adjuvant (Sigma). While for the first immunization the antigen was supplemented with complete adjuvant, the subsequent boosts included incomplete adjuvant. After three boosts, the serum (PoAb-aSOX_SUBDO) was collected and tested with a titer of 1:5,000. For controls, pre-immune serum had been taken from the same animal. This pre-immune serum did not cross-react with the immunogen.

SDS–PAGE AND WESTERN BLOT ANALYSES

SDS–PAGE was routinely performed as follows: 5 μg protein were dissolved in loading buffer (Roti-Load; Roth, Karlsruhe, Germany), boiled for 5 min, then subjected to SDS–PAGE (with 10% v/v polyacrylamide and 0.1% v/v SDS) as described [Laemmli, 1970]. Then, the gels were washed in 10% (v/v) methanol (supplemented with 7% v/v acetic acid) for 30 min. Finally, size-separated proteins were stained with Coomassie brilliant blue as described previously [Wiens et al., 1998]. Alternatively, size-separated proteins were transferred onto nitrocellulose membranes, using the iBlot system (Invitrogen). The membranes, then, were rinsed in TBS-T [20 mM Tris–HCl (pH 7.6), 137 mM NaCl, 0.1% v/v Tween-20] and incubated for 1 h with PoAb-aSOX_SUBDO; 1:1,000, as described earlier [Müller et al., 2005]. Following three additional washing steps with TBS-T, the membranes were incubated for 1 h with HRP-conjugated goat anti-rabbit IgG secondary antibody (Jackson ImmunoResearch, Newmarket, UK). For visualization of immunodetected proteins, the peroxidase substrate TMB (Linaris, Wertheim, Germany) was used.

IMMUNOHISTOLOGICAL ANALYSES

Tissue slices were prepared from specimens that had been kept for 3 days under continuous light exposure (a 25 $m^2/kg/s^3$ light bulb) and from specimens which had remained in complete darkness for the same period (controls). Samples were fixed in paraformaldehyde, embedded in Technovit 8100 (Heraeus Kulzer, Wehrheim, Germany), and sectioned as described [Müller et al., 2002]. The 5-μm thick slices were incubated overnight with either PoAb-aSOX_SUBDO (1:1,000 dilution), PoAb-aCRYPTO_SUBDO [1:1,000; Müller et al., 2010], or PoAb-aLUC_SUBDO [1:3,000; Müller et al., 2009]. Subsequently, the slices were treated with Cy3-conjugated donkey anti-rabbit immunoglobulin for 2 h and counterstained with 4'-6-diamidino-2-phenylindole (DAPI). Finally, slices were inspected with an Olympus AHBT3 microscope/Olympus IX-FLA Fluorescence Observation Attachment, using an excitation wavelength of 546 nm for the identification of Cy3-stained structures (red fluorescence) or of 350 nm for the analysis of DAPI-stained nucleic acids (blue). For light microscopic analyses, Nomarsky interference contrast optics were applied.

NORTHERN BLOTTING ANALYSES

At the indicated culture time, total RNA was isolated from *S. domuncula* tissue by TRIzol (Invitrogen) as outlined before [Müller et al., 2010]. Integrity of the isolated RNA was checked by the Experion automated electrophoresis system (Bio-Rad, Hercules, CA). Then, 5 μg of total RNA were size-separated through formaldehyde/agarose gel-electrophoresis and blotted onto Hybond N^+ membranes. Finally, hybridization (in DIG Easy Hyb solution; Roche, Mannheim, Germany) at 42°C was performed with one of the following probes (all derived of *S. domuncula* sequences), *SDSOX* (SOX-related protein; nt_{456} to nt_{913}) obtained by amplification with the primer pair Fwd: 5'-ACTTCAGCATACTCCATGCC-3'

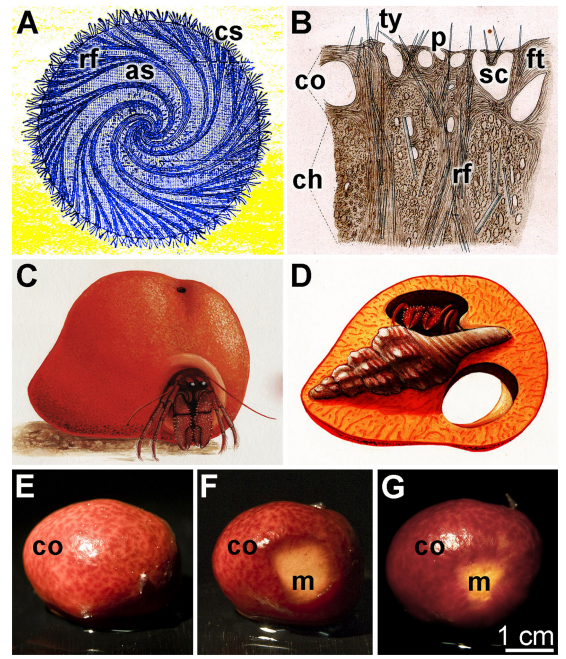

Fig. 1. Schematic representation of the skeletal organization in siliceous sponges (Demospongiae). A: "Radiate" pattern of the spiral type, the spicules are arranged in bundles that have been termed radiating skeletal fibers (rf). Within the fibers, tissue is organized and harbors the aquiferous canal system (as). At the surface of the animals, the radiating skeletal fibers splice into the individual cortical spicules (cs); from Ridley and Dendy [1887]. B: Cross-section through *Suberites perfectus*, displaying a more detailed description of the radial organization at the surface of this species [Ridley and Dendy, 1887]. The surface tissue is organized into the ectosome (co), which is layered on top of the choanosome (ch). The ectosome consists of brushes of nearly uniform spicules, tylostyles (ty). Individual spicules emerge from the radiating skeletal fibers (rf) and protrude into the surrounding milieu. Those spicules shelter pores (p) that function as ingestion openings for the aquiferous canal system. The pores lead to subdermal cavities (sc). The radiating skeletal fibers reinforce the fibrous tissue (ft) that is composed of individual cells embedded in a collagen network. C: Drawing of a *S. domuncula* specimen. D: Cross-section through *S. domuncula*, showing the hermit crab within a gastropod shell. E–G: A *S. domuncula* specimen prior to tissue ablation (E) and after 1 day of regeneration (F) of the removed cortical region (co). m, exposed medulla. Depth of the removed tissue, 2–3 mm. G: The same specimen after a regeneration time of 3 days. Newly regenerated cortical cell layers already partially cover the medulla beneath. [Color figure can be viewed in the online issue, which is available at wileyonlinelibrary.com]

(nt_{456} to nt_{475}) and Rev: 5'-GTATTGAGCGCAACTGATCC-3' (nt_{913} to nt_{893}), *SDLUC* (luciferase; FM201300; nt_{296} to nt_{875}) obtained with Fwd: 5'-ACCAGATTGACGAGTTGACA-3' (nt_{296} to nt_{315}) and Rev: 5'-CTGATGACTATCATGCCATAA-3' (nt_{875} to nt_{855}), *SDCRYPTO* (cryptochrome; FN421335; nt_{891} to nt_{1400}) obtained with the primer pairs Fwd: 5'-AGGACAAGAGCTCTTCGAAC-3' (nt_{891} to nt_{910}) and Rev: 5'-CACGGCTGATGAACATACTC-3' ($nt_{1,400}$ to $nt_{1,381}$), and finally the β-tubulin probe (*SDTUB*; AJ550806; nt_{772} to $nt_{1,229}$) with Fwd: 5'-AATGAGCGGAGTAACCACTTG-3' (nt_{772} to nt_{792}) and Rev: 5'-ACTGCTCGCTGATACGCTTG-3' ($nt_{1,229}$ to $nt_{1,210}$). DNA probes were synthesized by PCR, using the PCR DIG Probe Synthesis Kit (Roche) that facilitates incorporation of DIG-11-dUTP into the amplifying DNA strands. Hybridized DIG-labeled probes, then, were detected by successively applying anti-DIG antibodies (conjugated to alkaline phosphatase) and the enzyme substrate CDP-Star (Roche).

QUANTITATIVE REAL-TIME RT-PCR (QRT-PCR)

To remove possible DNA contamination from the extracted RNA, the samples (5 μg) were treated with 1 U of DNAse in RT buffer (20 μl) as described [Müller et al., 2010]. First-strand cDNA synthesis was performed by M-MLV reverse transcriptase (Promega, Madison, WI). Each reaction (40 μl) contained approximately 5 μg of total RNA, 0.5 mM dNTPs, 100 pmol of oligo$(dT)_{18}$, and 400 U reverse transcriptase in RT buffer. Reactions were incubated at 42°C for 1 h, followed by inactivation of the reverse transcriptase (65°C, 15 min). Subsequently, the quantitative real-time PCR (qPCR) experiments were performed in an iCycler (Bio-Rad), using 1/10 serial dilutions in triplicate, as described [Livak and Schmittgen, 2001; Velarde et al., 2009]. The reverse transcriptase reaction mixtures were diluted as required and 2 μl of the appropriate dilution were employed as a template for 30 μl qPCR assays. Each reaction contained "*Absolute* Blue *SYBR Green*" master mixture (ABgene, Hamburg, Germany) and 5 pmol of each primer. All reactions were run with an initial denaturation at 95°C for 3 min, followed by 40 cycles, each of 95°C for 20 s, 61°C for 20 s, 72°C for 20 s, and 80°C for 20 s. Fluorescence data were collected at the 80°C step. The following primers were used for amplification; *SDSOX* [Fwd: 5'-TGCTCCTCA-GATGATACCTGCC-3' (nt_{785} to nt_{806}) and Rev: 5'-TCTGTATT-GAGCGCAACTGATCC-3' (nt_{916} to nt_{894}); size of the fragment,

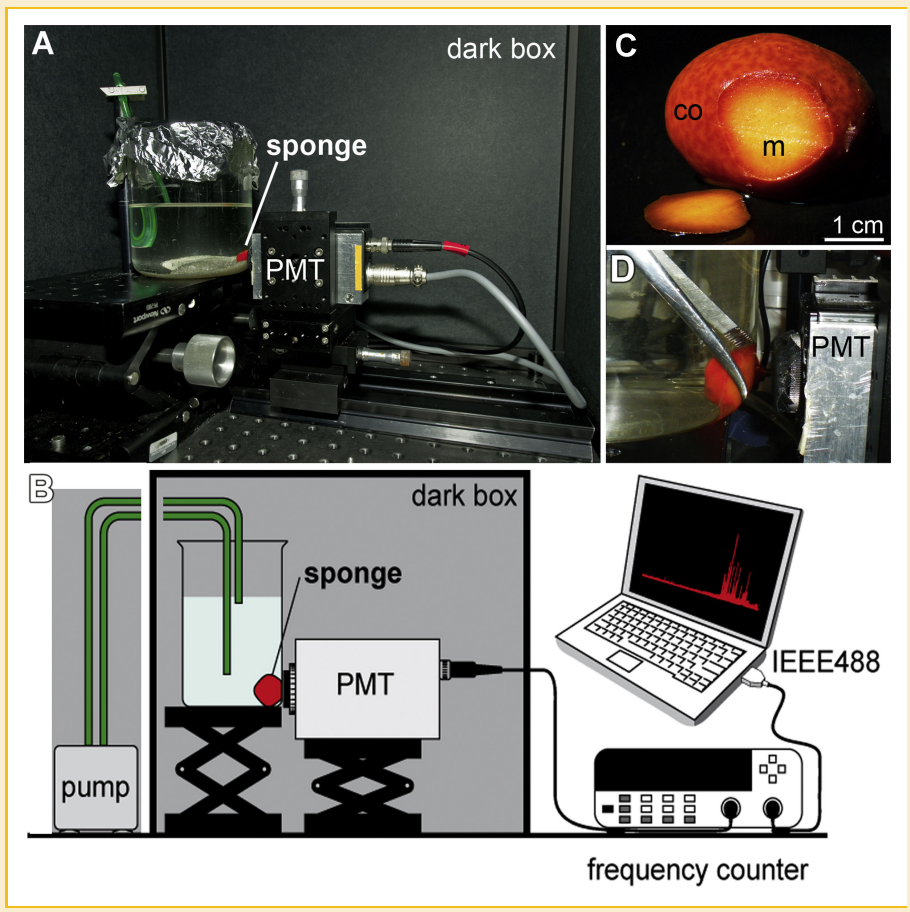

Fig. 2. The photon-measurement device. A: The photomultiplier tube (PMT) and the sponge specimen were placed in a vibration-free dark box. The sponge was kept under constant water circulation and fixed by means of a forceps, facing the PMT. B: Schematic representation of the PMT and the beaker with the sponge in the dark box. The data acquisition and processing devices were located outside of the box and consisted of the frequency counter, connected via *IEEE488* interface to a PC. C: From the specimen used for the measurements, the tissue surface layers, the cortex (co), had been ablated, exposing the underlying medulla (m). D: The animal was placed into the beaker so that the ablated surface faced the PMT. The image shows a fresh surface cut. [Color figure can be viewed in the online issue, which is available at wileyonlinelibrary.com]

132 bp], *SDCRYPTO* [Fwd: 5'-CCCTGTTTCGTCTGTTTGCTGG-3' ($nt_{1,227}$ to $nt_{1,248}$) and Rev: 5'-CGGCTGATGAACATACTCG-GAAGG-3' ($nt_{1,398}$ to $nt_{1,375}$); size, 172 bp], *SDLUC* [Fwd: 5'-GGTGACAAACTTGCTCGCTTGG-3' (nt_{734} to nt_{755}) and Rev: 5'-AAATTCCTCCCGCGTTTGGCTC-3' (nt_{881} to nt_{860}); size, 148 bp], and finally *SDTUB* [Fwd: 5'-AACCGCTGTTTGCGACATCC-3' ($nt_{1,126}$ to $nt_{1,145}$) and Rev: 5'-CAATGCAAGAAAGCCTTTCGCC-3' ($nt_{1,266}$ to $nt_{1,245}$); size, 141 bp]. The threshold position was set to 50.0 RFU above PCR subtracted baseline for all runs. Mean C_t values and efficiencies were calculated by the iCycler software (Bio-Rad). The estimated PCR efficiencies were in a range of 92–103%. Expression levels of the respective transcripts (SDSOX, *SDLUC*, and *SDCRYPTO*) to tubulin (*SDTUB*) were correlated to determine relative expression levels (e.g., $E_{Tub}^{CtTub}/E_{Cry}^{CtCry}$) where "E" describes PCR efficiency and "C_t" represents the threshold cycle [Pfaffl, 2001].

FURTHER METHODS

For protein quantification, the Bradford method was used [Compton and Jones, 1985; Roti-Quant, Roth). For statistical analyses, the calculation of mean values and standard error of the mean (SEM), the described procedure was applied [Sachs, 1984].

RESULTS

COMPLEX AND ORGANIZED ARRANGEMENT OF SILICEOUS SPICULES

The spicule-based skeleton of sponges is architecturally complex and arranged in a functionally efficient way. As already outlined in the Challenger Report [Ridley and Dendy, 1887], two main types of spicule arrangements are realized in demosponges, the "Reticulate" and the "Radiate." The arrangement of these spicules follows a genetically determined pattern, which is either radial or spiral. The spiral organization is characteristic, for example, for the Tethyidae (Fig. 1A) and the radial skeleton, for example, for the Suberitidae (Fig. 1B). *S. domuncula* lives in a community with a hermit crab that, in turn, resides within a gastropod shell (Fig. 1C,D). The central as well as the peripheral skeleton of *S. domuncula* is composed of spicules that are oriented along the aquiferous canal system (Fig. 1B).

ABLATION OF SURFACE CELL LAYERS

For the studies described here, immobile specimens without hermit crabs were selected (Fig. 1E). Subsequently, surface tissue was removed, mainly the reddish cortex, revealing the underlying yellowish medulla (Fig. 1F). After 3 days in culture, re-growing cortex cell layers seal the exposed medullar region again (Fig. 1G). This process, the rapid regeneration of damaged tissue, is a characteristic feature of sponges and bases on their high regeneration capacity due to the presence of pluripotent stem cells [Müller, 2006]. The surface layer is rich in spicules and in cells that express *luciferase* [Müller et al., 2009] and *cryptochrome* [Müller et al., 2010]. Thus, ablation of surface tissue induced two processes; firstly the reconstitution of skeletal elements and fibrous tissue, and secondly the differentiation of proliferating cells into cells that express the proteins luciferase and cryptochrome.

LIGHT GENERATION BY DARK-ADAPTED SPONGE SPECIMENS

After ablation of cortical cell layers (Fig. 2C), dark-adapted specimens without hermit crabs were immediately placed into a beaker with seawater that was under constant aeration. Then, the beaker was positioned in a padded dark box, with the freshly cut sponge surface as close as possible to the photomultiplier tube (PMT; Fig. 2A,B). The PMT was connected in series with a frequency counter and data acquisition unit outside the box. The specimen was fixed in position with a forceps (Fig. 2D). Light (photon) emission was recorded within a range of 300–890 nm. The dark count rate of the detector was 10/s and, therefore, around one dark count per measuring interval. The quantum efficiency (QE) of the detector was 15% in the range of visible wavelengths. The counting rate was close to 100%. Based on these properties, detection was limited to around 100 emitted photons.

During a typical experiment, the sponge specimens started to emit light after a lag phase of 1,400–2,000 min (23–33 h). A characteristic recording profile is shown in Figure 3. In this experiment, the specimen started to flash after 1,688 min of complete inactivity. Almost at the onset of flashing the highest number of counts (2,250 counts) was recorded. The activity lasted until ca. 4,000 min (66 h).

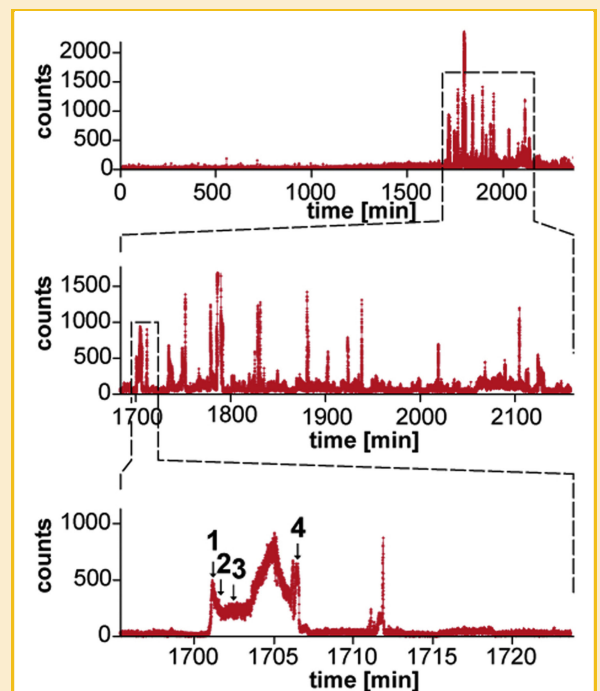

Fig. 3. Light generation/flashing by *S. domuncula*. Typically, flashing started after a lag phase of 1,400–2,000 min. In the representative experiment shown here the first signals (counts, reflecting the photon intensities) were recorded after a period of 1,688 min. The strongest signals were detected until approximately 1,900 min, from beginning of the experiment. Magnification of the peaks revealed a characteristic shape; one multi-peak flash sequence is shown between 1,702 and 1,707 min. Such a typical flashing can be divided into an initial strong burst (1), followed by an exponential decrease (2), which then enters a short plateau phase (3); one flash unit ends with a sudden end (4). [Color figure can be viewed in the online issue, which is available at wileyonlinelibrary.com]

This observation was a first indicator that flashing of the sponge specimens correlated with the onset of cortical cell regeneration (Fig. 1F,G). Magnification of the recorded flashes revealed a characteristic shape, with an initial and major—perhaps overshooting—burst, followed by a (bi)exponential decrease, passing into a plateau phase. At times, this pattern was immediately repeated. Finally, the flashing activity was abruptly terminated, as indicated by a sudden drop in the number of counts detected (Fig. 3; lower panel).

S. DOMUNCULA SOX-RELATED PROTEIN: SEQUENCE ANALYSIS AND PHYLOGENETIC RELATIONSHIPS

A fragment of the *S. domuncula* SOX-related protein was initially identified by in silico screening of a poriferan EST (expressed sequence tag) database. The sequence, then, was completed through primer-walking with a standard *S. domuncula* cDNA library as template. The complete *SDSOX* sequence comprises 1,061 nts, with an ORF between nt_{177} and $nt_{1,061}$ that encodes the putative protein SOX_SUBDO (Fig. 4A). SOX_SUBDO has a predicted size of 31,660 Da and an isoelectric point (pI) of 9.87. Similar to its related metazoan family members [Koopman et al., 2004], the poriferan SOX-related protein also comprises a HMG domain (Prosite accession number PS50118) from aa_{11} to aa_{79} (Fig. 4A). The corresponding E-value of $3 \times 6e-34$ reflects high significance [Coligan et al., 2000]. The HMG domain represents a DNA-binding motif, which is found in specific regulators of transcription and cell differentiation [Grosschedl et al., 1994]. HMG domain proteins primarily interact with the minor groove of the DNA helix, concurrently facilitating protein-induced DNA bending, a process that is driven by the three α-helices of the domain. HMG domain proteins can be divided into several subfamilies, including the yeast mating-type genes (MATA), the T-cell transcription factors (TCF), and the Sry-related genes (SOX) [Soullier et al., 1999]. The poriferan HMG domain shares significant sequence similarity to the vertebrate

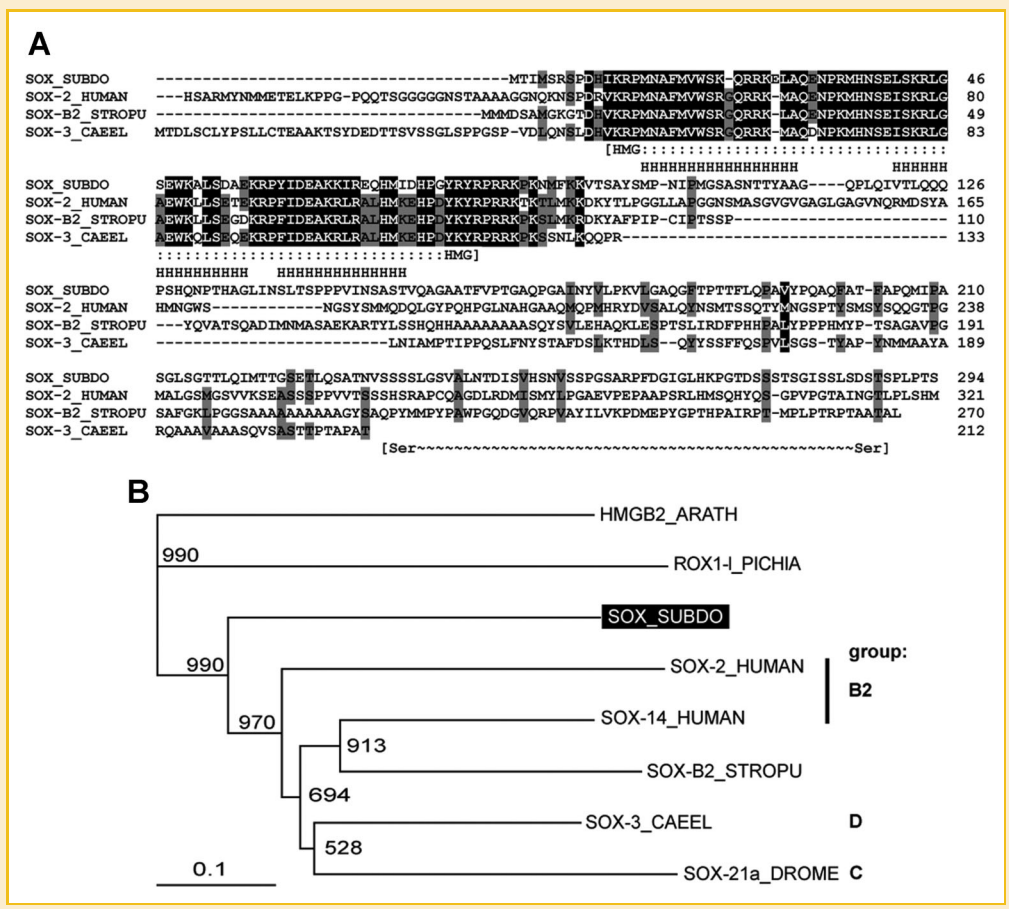

Fig. 4. *S. domuncula* SOX-related protein. A: The deduced poriferan SOX-related protein sequence SOX_SUBDO (*S. domuncula*) was aligned with three related metazoan SOX proteins, human SOX-2 (SOX-2_HUMAN; NP_003097.1), *Strongylocentrotus purpuratus* SOX-B2 (SOX-B2_STROPU; ABI53364.1), and *Caenorhabditis elegans* SOX-3 (SOX-3_CAEEL; NP_510439.1). Residues conserved (identical or similar with respect to their physico-chemical properties) in all sequences are shown in white on black; those that share similarity in three sequences are in black on gray. The characteristic domains, the HMG box (HMG::HMG), the three α-helix stretches within the HMG domain (HHHHH), and the Ser-stretch of poriferan and human protein (Ser∼∼∼Ser) are marked. B: For phylogenetic analyses the aforementioned sequences were used together with the following molecules: human SOX-14 (SOX-14_HUMAN; NP_004180.1), *Drosophila melanogaster* SOX-21a (SOX-21a_DROME; NP_648694.1), *Pichia stipitis* ROX1-I HMG-box transcription factor (ROX1-I_PICHIA; XP_001383328.2), and *Arabidopsis thaliana* High Mobility Group B-2 (HMGB2_ARATH; NP_001077569.1). The latter sequence was used to root the tree. The degree of support of internal branches was assessed by bootstrapping (1,000 replicates) and the evolutionary distance calculated (0.1 aa substitutions per position in the sequence). The relevant classification into groups is indicated.

SOX TFs, revealing only lower similarity to protostomian HMG domains [Laudet et al., 1993; Soullier et al., 1999]. Since the poriferan SOX protein comprises only a single HMG domain, a specific interaction with defined nucleotide sequences can be assumed [Grosschedl et al., 1994].

The homology of the poriferan SOX protein to other metazoan family members is significant. Thus, the similarity/identity of SOX_SUBDO to human SOX-2 (SOX-2_HUMAN; NP_003097.1; Fig. 4B) is particularly high with 36%/22%. In contrast, the values to other human or metazoan SOX proteins are somewhat lower, for example, human SOX-14 (SOX-14_HUMAN; NP_004180.1; 31%/19%) or sea urchin SOX-B2 (SOX-B2 _STROPU; ABI53364.1, 30%/17%). In this context, similarity/identity to SOX-3 of *Caenorhabditis elegans* (SOX-3_CAEEL; NP_510439.1) is quite low with 29%/19%, whereas homology to yeast ROX-1 (*Pichia stipitis*; ROX1-l_PICHIA; XP_001383328.2) and plant High Mobility Group B-2 molecule (*Arabidopsis thaliana*; HMGB2_ARATH; NP_001077569.1) is poor, with scores around 17%/8%. A rooted phylogenetic tree demonstrates these relationships and reveals the poriferan molecule at the basis of the metazoan SOX family (Fig. 4B). The close relationship between SOX_SUBDO and human SOX-2 can also be deduced from the fact that only these two sequences share a serine-rich region profile (aa_{235} to aa_{289} in the poriferan protein; Prosite accession number PS50324). In earlier studies, it has been reported that the *S. domuncula* luciferase represents the ancestor of all metazoan enzymes of that kind (Müller et al., 2009). Focusing on the sponge cryptochrome, this protein formed the basis of the diploplasts/vertebrates cryptochromes (Müller et al., 2010).

S. DOMUNCULA SOX-RELATED PROTEIN: RECOMBINANT PROTEIN AND ANTIBODIES

The cDNA coding for the sponge SOX-related protein (*SDSOX*) was expressed in *E. coli*. After induction with IPTG, the recombinant protein carrying a C-terminal 6xHis-tag, was purified by Ni-IDA affinity chromatography, resulting in one band on the SDS gel that corresponds to the calculated size of the 35-kDa fusion (Fig. 5A, lane c). In untransformed control cells, this band is not seen (lane a), while the recombinant protein is already visible in crude extracts of the IPTG-induced bacterial cells (lane b). Then, the purified protein was employed to raise antibodies in rabbits. On Western blots, the resulting polyclonal antiserum (PoAb-aSOX_SUBDO) successfully detected the recombinant SOX-related protein (Fig. 5B, lane a), while pre-immune serum did not cross-react (lane b).

EXPRESSION STUDIES: IMMUNOHISTOLOGICAL ANALYSES

Sponge specimens were exposed to laboratory light for 3 days. Then, tissue sections were prepared for immunohistological analysis of expression and localization of luciferase, cryptochrome, and SOX-related protein, using PoAb-aLUC_SUBDO, PoAb-aCRYPTO_-SUBDO, and PoAb-aSOX_SUBDO, respectively. Resulting immunocomplexes were detected with Cy3-conjugated secondary antibodies. Fluorescence microscopy of the immunostained sections of light-exposed specimens showed in all three cases a clear and, even more, a distinct regional staining pattern (Fig. 6). Thus, in the case of the luciferase, brightest fluorescence was seen in the upper 500-μm thick cortical layers (Fig. 6A); their a dense accumulation of

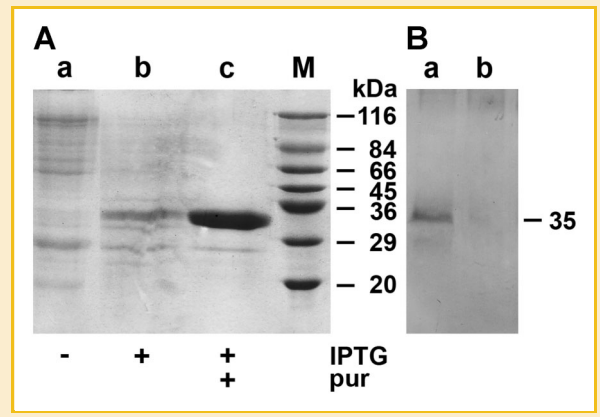

Fig. 5. Preparation of recombinant SOX-related polypeptide. A: *E. coli* had been transformed with the cDNA coding for the SOX-related polypeptide (*SDSOX*). Bacteria remained either non-induced (−; lane a) or were treated with IPTG (+ IPTG; lane b). The recombinant protein was isolated and subsequently purified (+ pur) from the induced cultures. B: The purified recombinant protein was used to raise polyclonal antibodies (PoAb-aSOX_-SUBDO). On Western blots this antiserum detected the recombinant 35 kDa SOX protein (lane a). The pre-immune serum did not elicit cross reactions (lane b). M, size marker

tylostyle spicules occurred. Immunohistological staining of cryptochrome revealed a similar regional distribution pattern. Again, the surface region was brightly stained (Fig. 6D). The same slices were microscopically examined by Nomarski interference contrast to visualize cell localization (Fig. 6B,E). With PoAb-aSOX_SUBDO, in contrast, the immunofluorescence signals obtained were comparably weak. In addition, the signals were restricted to a thin cell layer (50–70 μm in thickness) at the surface of the specimens (Fig. 6G). Figure 6J depicts a similar region at higher magnification. The same slides were analyzed for their DAPI-stained cell nuclei (Fig. 6H,K).

In a parallel set of control experiments, tissue sections of dark-adapted sponge specimens (3 days) were reacted with the respective immune sera. In all approaches, immunocomplexes were barely detectable, neither in the case of the luciferase antiserum (Fig. 6C), nor for cryptochrome (Fig. 6F) or the SOX-related protein (Fig. 6I,L).

EXPRESSION STUDIES: NORTHERN BLOT AND REAL-TIME RT-PCR ANALYSES

Animals were subjected to tissue ablation of the cortex region, as described under "Materials and Methods Section." Then, tissue samples were taken from the resulting surface layers of the animal at intervals of 6–30 h and to a depth of 2–3 mm. At the beginning of the experiments (time 0 h), tissue of the medulla, just below the ablated cortical region was taken. At later phases, newly formed cortex tissue was increasingly included in the extraction, due to the ongoing regeneration of the formerly damaged tissue. Then, RNA was isolated, size-separated, and blotted onto nylon membranes. Subsequently, the membranes were incubated with DIG-labeled probes. Whereas in RNA of dark-adapted specimens neither probe elicited specific signals, in light-exposed specimens the respective transcripts of *SOX-related protein*, *luciferase*, and *cryptochrome* were detected (Fig. 7). Thus, the first signals of the *SOX-related*

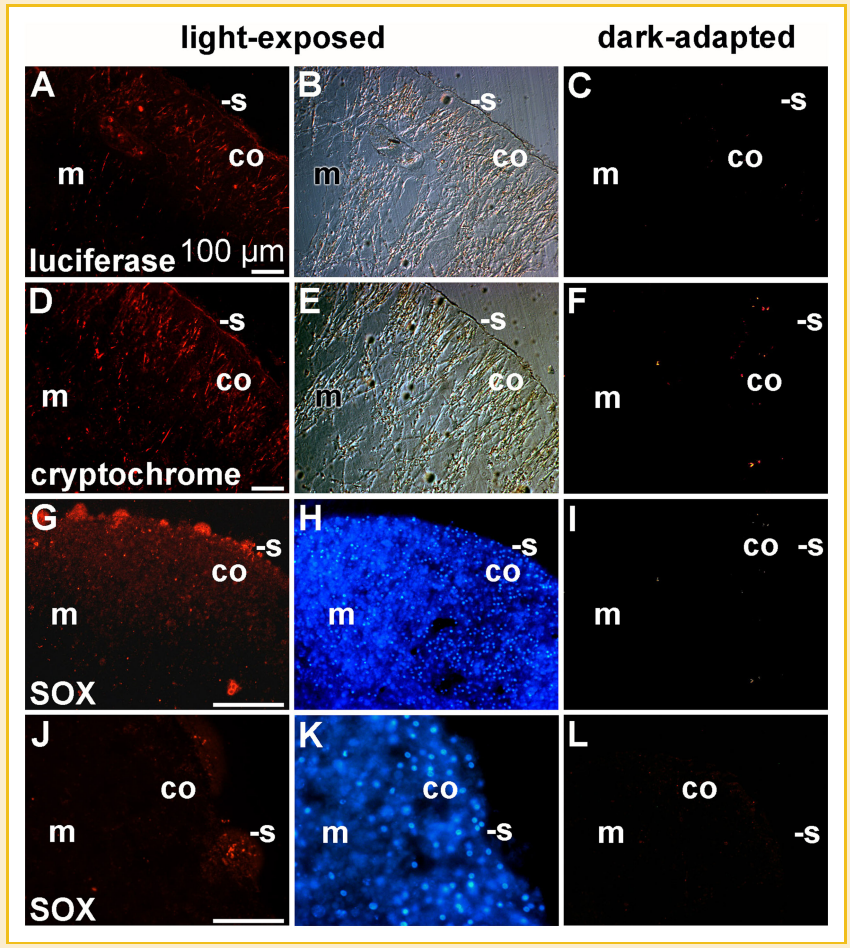

Fig. 6. Light-dependent protein expression and localization of luciferase, cryptochrome, and SOX-related protein in sponge tissue. The tissue slices were reacted with the following antibodies: (A) PoAb-aLUC_SUBDO (luciferase), (D) PoAb-aCRYPTO_SUBDO (cryptochrome) or (G and J) PoAb-aSOX_SUBDO (SOX-related protein). Immunocomplexes were visualized with Cy3-conjugated anti-rabbit secondary antibodies under fluorescent light. In parallel, sections were analyzed by Nomarski interference contrast (B and E) or by fluorescent light after staining with DAPI (H and K). In a set of control experiments, tissue slices of dark-adapted sponges were reacted with the same antisera: (C) PoAb-aLUC_SUBDO, (F) PoAb-aCRYPTO_SUBDO, (I and L) PoAb-aSOX_SUBDO. Sponge surface (s), cortex (co), and medulla (m) are marked. Size bars: 100 µm. [Color figure can be viewed in the online issue, which is available at wileyonlinelibrary.com]

protein were seen as early as 6 h following tissue ablation and continuously increased in strength until 18 h. In contrast, the first recognizable transcripts of *luciferase* appeared only after 12 h, steadily increasing in strength afterwards until the end of the experiment (30 h). Even more delayed the first *cryptochrome* transcripts were detected, after 18 h. At the highest expression level of luciferase and cryptochrome (30 h post-ablation), transcripts of *SOX-related protein* were no longer detectable. The expression of tubulin was used as internal control and remained almost constant throughout the experiment.

To substantiate the semi-quantitative results obtained by Northern blot analyses, the technique of qRT-PCR was applied to the abovementioned RNA samples. The data show that first transcripts of *SOX-related protein* can be detected 6 h after ablation until a maximal expression level is reached after 18 h ($(mRNA_{SOX} \pm SEM)/mRNA_{tub} = (14.2 \pm 1.8) \times 10^{-5}$; Table I). Higher expression levels (also correlated to the *β-tubulin* expression) were determined for *luciferase* $[(87 \pm 11) \times 10^{-5}]$ and *cryptochrome* $[(174 \pm 21) \times 10^{-5}]$. In contrast to the transcripts of the *SOX-related protein* that could no longer be detected after 30 h, a steadily increased expression of *luciferase* and *cryptochrome* was observed until the end of the study (Table I).

EXPRESSION STUDIES AT DIFFERENT LIGHT: NORTHERN BLOT ANALYSES

In order to assess whether the expression of the *SOX-related protein* gene in the animals depended on different light spectra they were exposed to blue light [using a filter with a lower cut off wavelength of 300 nm (maximum at >400 nm)], green light [lower cut off at 400 nm (maximum at 520 nm)], or red light [lower cut off at 500 nm (maximum at >650 nm)]. After incubation (0–24 h) tissue slices from surfaces of the animals were taken and RNA was extracted. The steady-state expression of the gene encoding the *SOX-related protein* was analyzed by Northern blot analysis. The data showed that the highest transcription level was seen in tissue from animals that were exposed to blue light (high levels are seen after 12 and 24 h); less lasting was the expression in animals exposed to red light (transient expression after 12 h); Figure 8. No transcripts of

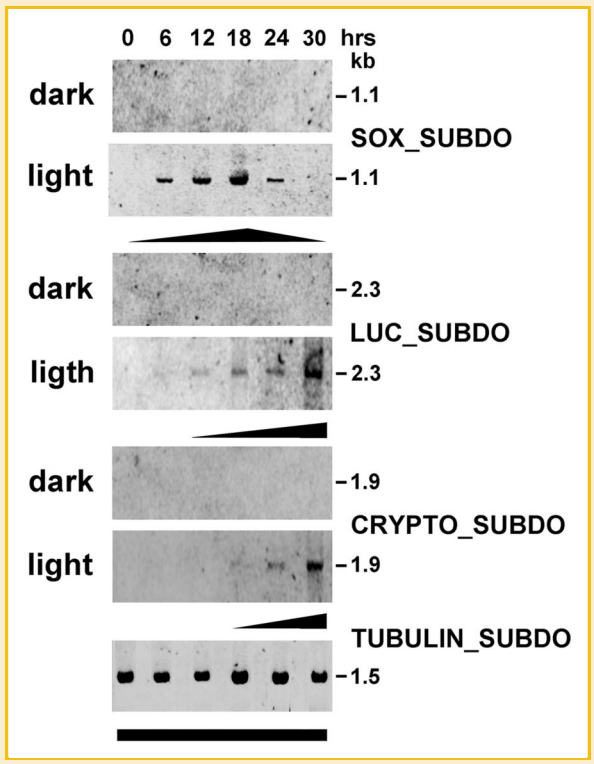

Fig. 7. Differential gene expression in *S. domuncula* tissue of SOX-related protein (SOX_SUBDO), luciferase (LUC_SUBDO), cryptochrome (CRYPTO_-SUBDO), and the house-keeping molecule β-tubulin (TUBULIN_SUBDO). The surface layers, the cortex, had been removed. Then, the animals had been kept in the dark or had been exposed to light. At the indicated time, samples were taken from the regenerating tissue. At time 0, tissue from the medulla was sampled. Subsequently, RNA was extracted, size-separated, blotted, and hybridized with DIG-labeled probes of *SDSOX* (SOX-related protein), *SDLUC* (luciferase), or *SDCRYPTO* (cryptochrome). To confirm that same amounts of RNA were loaded onto the gels, size-separated RNA was probed for transcripts of the gene *β-tubulin*. Transcript sizes are indicated. Bars or polygons below the blots depict the relative expression level of the respective transcripts.

SOX-related protein could be detected in tissue from animals that remained in the dark or were illuminated with red light (Fig. 8). Again, the amount of *tubulin* transcripts was determined to ensure that the same amount of RNA had been loaded onto the gel.

TABLE I. Expression Levels of Poriferan SOX-Related Protein, Luciferase, and Cryptochrome

	Gene expression: $(mRNA_x \pm SEM)/mRNA_{tub}$		
Time point (h)	SOX-related protein	Luciferase	Cryptochrome
0	Below detection limit	Below detection limit	Below detection limit
6	$(1.3 \pm 0.2) \times 10^{-5}$	$(7 \pm 1) \times 10^{-5}$	Below detection limit
12	$(6.0 \pm 0.1) \times 10^{-5}$	$(12 \pm 2) \times 10^{-5}$	$(62 \pm 9) \times 10^{-5}$
18	$(14.2 \pm 1.8) \times 10^{-5}$	$(87 \pm 11) \times 10^{-5}$	$(174 \pm 21) \times 10^{-5}$
24	$(2.1 \pm 0.3) \times 10^{-5}$	$(291 \pm 31) \times 10^{-5}$	$(832 \pm 64) \times 10^{-5}$
30	Below detection limit	$(423 \pm 47) \times 10^{-5}$	$(1520 \pm 138) \times 10^{-5}$

Expression was quantified through qRT-PCR. Each data point represents the mRNA amount of the respective gene (x) normalized to the amount of *β-tubulin* transcripts, as means ± SEM (n = five experiments per time point).

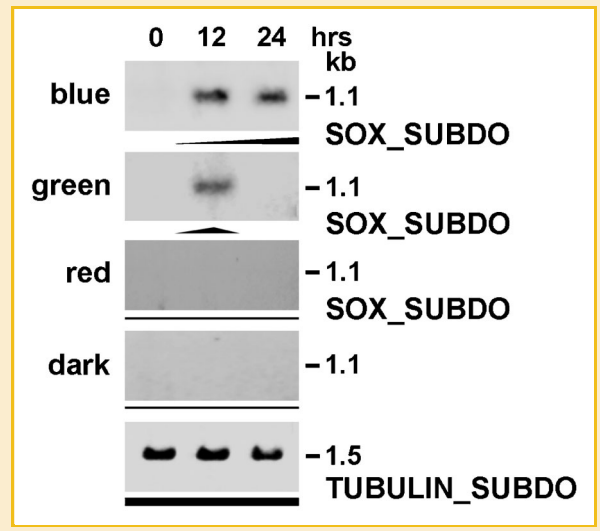

Fig. 8. Expression of the gene encoding the SOX-related protein (SOX_-SUBDO). Animals were exposed to blue, green or red light, or remained in the dark for 0–24 h, as outlined under "Materials and Methods" Section. Then tissue samples were taken from the surface of the animals; after RNA extraction Northern blot analysis was performed using the DIG-labeled *SDSOX* probe. The expression level of *β-tubulin* was determined to ensure that the amount of RNA per slot was comparable.

DISCUSSION

The proposed phototransduction/-reception system of siliceous sponges, with the demosponge *S. domuncula* as animal model organism, comprises three components, (i) light-generating enzyme (i.e., luciferase; [Müller et al., 2009]), (ii) light waveguides (i.e., siliceous spicules [Aizenberg et al., 2004; Müller et al., 2006]), and (iii) photoreceptor (i.e., cryptochrome [Müller et al., 2010]). In *S. domuncula*, these components are predominantly localized in the sponge surface region, the cortex [Müller et al., 2009, 2010]. Accordingly, for the present study, the cortical cell layers were removed and analyzed. For this purpose, the time-dependent reconstitution of the proteinaceous components—effector (elicitor) and receptor (receiver)—was determined in regenerating cortical tissue. To account for differential expression patterns, this study concurrently focused on the search for poriferan TF, potentially involved in upstream regulation of expression of luciferase and cryptochrome, including Pax-6. Pax-6 is essentially involved in development of eyes and sensory organs [Gehring and Ikeo, 2009]. However, irrespective of the most intensive screening efforts in our laboratories, no Pax-6 homolog has been identified in demosponges (*S. domuncula* and *Lubomirskia baicalensis*) so far. This initiated a search for another putative master control gene involved in development of the proposed *S. domuncula* photosystem, that is, a SOX-related protein. Previously, it had been outlined that members of the family of SOX TF, especially SOX-2, are crucially involved in transcriptional activation during early vertebrate eye and brain development [Hagstrom et al., 2005]. In this context, it is interesting to note that SOX-2 and Pax-6 form a DNA-binding complex that regulates, for example, development of the vertebrate lens. The

search for a poriferan candidate molecule has resulted in the identification of a single SOX-related protein (SOX_SUBDO). Subsequent bioinformatic comparative analyses, including more than 30 different metazoan orthologous genes that have been described so far [Wegner, 1999; Koopman et al., 2004], revealed the characteristic and highly conserved DNA-binding domain, the HMG box [Grosschedl et al., 1994; Soullier et al., 1999], which is present in a number of regulators of transcription and cell differentiation. Corresponding phylogenetic analysis demonstrated that SOX_SUBDO shares indeed the highest sequence similarity to vertebrate SOX-2, with which it also has an extensive Ser-rich stretch in common. Based on these data, SOX_SUBDO can be considered as a candidate TF that is involved in the upstream regulation of the putative poriferan photosensory system. To substantiate this hypothesis, recombinant protein was prepared and used to raise PoAb against the 35 kDa protein. Subsequently, these antibodies were employed to determine the regional gene expression pattern in sponge tissue. This mapping analysis indicated that maximal expression of the SOX-related protein occurs at the animal surface. There, SOX is concentrated in small hillocks (size $20 \times 20\ \mu m$) that seem to bud from the pinacoderm (the outermost layer of cells). Concurrent immunolocalization studies of luciferase and cryptochrome revealed a predominant colocalization of the three proteins in the surface layers of sponge tissue that had been exposed to light. In contrast, in the tissue of dark-adapted specimens the respective proteins were not (or barely) detectable, consequently indicating a light-controlled expression of *SOX-related protein*, *luciferase*, and *cryptochrome*.

Light-responsive, spatially restricted expression of these proteins subsequently stimulated the analysis of time-dependent expression patterns during regeneration/reconstitution of damaged surface tissue. It is well-known that tissue regeneration in *S. domuncula*, for example, studied during the process of autograft fusion, is a fast process. Thus, transplants with a surface of ca. 2 cm^2 usually fuse completely within 3 days [Müller et al., 2002]. In the present study, the damaged sponge surfaces start to reconstitute already during the first 24 h post-intervention; after approximately 3 days, the regeneration process is terminated.

Since the time required for induction of gene expression is usually shorter than 24 h, the first 30 h (in intervals of 6 h) after tissue ablation were chosen to investigate transcription of *SOX-related protein*, *luciferase*, and *cryptochrome*. In both cases, semi-quantitative Northern blot analyses and qRT-PCR, the expression levels of all candidates was below detection limit in dark-adapted sponge specimens. Similarly, at the beginning of the experiments (time 0 h), no transcripts were detected in the medullar region, just below the ablated cortical tissue. Already 6 h post-ablation, the first signals reflecting the presence of measurable levels of transcripts were seen. At that time, the relative expression level of the *SOX-related protein* was highest (10% of the maximum level), while expression of *luciferase* and *cryptochrome* were lower (1–2%) or below the detection limit, respectively. After 18 h, *SOX-related protein* expression peaked and, then, dropped rapidly to a non-detectable level at 30 h. In contrast, the transcription of *luciferase* continuously increased until the end of the observation period, almost in parallel, with a delay of 6 h, with the expression of *cryptochrome*. Based on these data, a time-dependent expression pattern, triggered by tissue ablation, can be deduced: *SOX* > *luciferase* > *cryptochrome*. This pattern inversely correlates with the relative amount of transcripts detected, in comparison to the tubulin

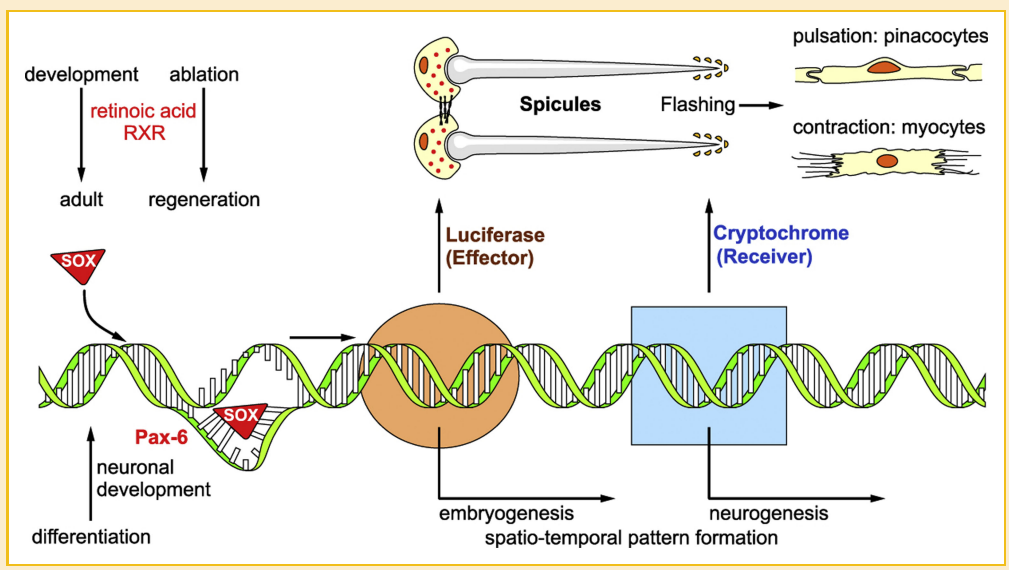

Fig. 9. Proposed light-flashing signaling circuit in the sponge *S. domuncula*. During development and regeneration of sponge tissue, binding of the morphogen retinoic acid to its receptor RXR induces expression of the transcription factor, the SOX-related protein (SOX). In vertebrates SOX operates during differentiation in general and neuronal development in particular. Flanked by Pax-6, a TF without apparent poriferan homolog, SOX-2 causes coordinated development of cells during embryogenesis and neurogenesis. In sponges the SOX-related protein causes consecutive expression of luciferase (effector) and cryptochrome (receiver). Both are components of the poriferan light generating/harvesting system, also including siliceous spicules as light waveguides. In this manner, coordinated transmitted signals might regulate, for example, pulsation of pinacocytes or contraction of myocytes. [Color figure can be viewed in the online issue, which is available at wileyonlinelibrary.com]

expression: *SOX* < *luciferase* < *cryptochrome*. This phenomenon is indicative for a cascade-like reaction, during which the transmitted signal is amplified. In a parallel series of experiments the animals were exposed to blue, green, or red light in order to determine the maximal susceptibility of the animals for light of different wavelengths. Highest expression levels for gene encoding the *SOX-related protein* were determined in tissue from animals exposed to blue light; also illumination with red light resulted in a response, however, less pronounced. Keeping at red light or in the dark caused no expression of the gene (*SOX*).

The hitherto discussed results suggest that the poriferan SOX-related protein controls processes during development/regeneration of tissue, a well-established function of the vertebrate molecule [Koopman et al., 2004; Hagstrom et al., 2005]. Initial experiments have shown that expression of vertebrate SOX-2 is not controlled by the organizer factors, fibroblast growth factor FGF4 and chordin [Streit and Stern, 1999]. Furthermore, SOX-2 has been proposed to work synergistically with FGF in signaling processes that initiate neural induction. Later experimental evidence indicated that FGF2 induces *SOX-2* expression [Mansukhani et al., 2005]. A different attractive route to shed light on the inducer(s) of *SOX* expression was shown by the work of Stevanovic [2003], demonstrating the effect of retinoic acid (RA) on neural differentiation of NTERA2 cells. RA and its poriferan receptor had previously been studied by authors [Biesalski et al., 1992; Wiens et al., 2003]. In addition, a role of RA was proposed as morphogen during aggregation of dissociated sponge cells to primmorphs [Imsiecke et al., 1994; Wiens et al., 2003]. The combination with the data of the present study suggests that RA induces morphogenetic events, which proceed very early in the differentiation of cell lineages from pluripotent stem cells [Müller, 2006]; summarized schematically in Figure 9.

After reconstitution of the cortex and the phase-dependent expression of the building blocks of the proposed photosystem, sponges start to generate light impulses. During the first 28 h post-ablation of surface tissue only short, weak, and rare flashes occur. This period of dormancy is terminated by heavy activity. During the subsequent 10 h of observation peaks were recorded with up to 2,250 counts. At present, it is only possible to speculate about the function of the proposed light flashing/signaling circuit during reconstitution of damaged poriferan tissue. In earlier reports, it had been proposed that in corals the light-responsive cryptochrome system is involved in the synchronization of, for example, mass spawning [Levy et al., 2003], concurrently suggesting that the coral cryptochrome system controls an ancient circadian clock-related rhythm. Similarly, *S. domuncula* cryptochrome was proposed to operate as a light-harvesting system, facilitating collection and transduction of environmental light [Müller et al., 2010]. Alternatively, poriferan cryptochrome has been implicated in the detection of biogenous light, emitted during a luciferase-catalyzed reaction [Müller et al., 2010]. The data of the present study substantiate the presence of an endogenous light signaling system in sponges, with luciferase as effector and cryptochrome as receiver. This light signal transmission could be involved in contraction/expansion of the poriferan aquiferous system [Nickel, 2006]. The underlying cellular elements include (i) pinacocytes that are the functional pacemakers of the contraction/expansion rhythm [Pavans de Ceccatty, 1989] and (ii) myocytes that provide the required contractile filaments [Prosser et al., 1962]; see scheme in Figure 9.

In conclusion, the data presented here suggest that, similar to corals, sponges are provided with a photosystem that controls distinct behavioral patterns and physiological reactions (e.g., rhythmic pulsations of aquiferous canals in the sponge body). The implication of the poriferan light sensory systems in a general endogenous circadian rhythm will be the subject for future investigations.

DATABASE

The SOX-related/similarity protein sequence from *Suberites domuncula* (SOX_SUBDO; accession number FN689551) has been deposited (EMBL/GenBank).

REFERENCES

Aizenberg J, Sundar V, Yablon AD, Weaver JC, Chen G. 2004. Biological glass fibers: Correlation between optical and structural properties. Proc Natl Acad Sci USA 101:3358–3363.

Biesalski HK, Doepner G, Tzimas G, Gamulin V, Schröder HC, Batel R, Nau H, Müller WEG. 1992. Modulation of myb gene expression in sponges by retinoic acid. Oncogene 7:1765–1774.

Cattaneo-Vietti R, Bavestrello G, Cerrano C, Sarà A, Benatti U, Giovine M, Gaino E. 1996. Optical fibres in an Antarctic sponge. Nature 383:397–398.

Coligan JE, Dunn BM, Ploegh HL, Speicher DW, Wingfield PT. 2000. Current protocols in protein science. Chichester: John Wiley & Sons. pp 2.0.1–2.8.17.

Compton S, Jones CG. 1985. Mechanism of dye response and interference in the Bradford protein assay. Anal Biochem 151:369–374.

Elliott GRD, Leys SP. 2007. Coordinated contractions effectively expel water from the aquiferous system of a freshwater sponge. J Exp Biol 210:3736–3748.

Felsenstein J. 1993. PHYLIP, ver. 3.5. Seattle: University of Washington.

Gehring WJ, Ikeo K. 2009. Pax 6: Mastering eye morphogenesis and eye evolution. Trends Genet 15:371–377.

Grosschedl R, Giese K, Pagel J. 1994. HMG domain proteins: Architectural elements in the assembly of nucleoprotein structures. Trends Genet 10:94–100.

Hagstrom SA, Pauer GJ, Reid J, Simpson E, Crowe S, Maumenee IH, Traboulsi EI. 2005. SOX2 mutation causes anophthalmia, hearing loss, and brain anomalies. Am J Med Genet 138A:95–98.

Harvey EN. 1921. Studies on bioluminescence. XIII. Luminescence in the coelenterates. Biol Bull 41:280–284.

Imsiecke G, Borojevic R, Müller WEG. 1994. Retinoic acid acts as a morphogen in freshwater sponges. Invertebr Reprod Dev 26:89–98.

Koopman P, Schepers G, Brenner S, Venkatesh B. 2004. Origin and diversity of the Sox transcription factor gene family: Genome-wide analysis in *Fugu rubripes*. Gene 328:177–186.

Laemmli UK. 1970. Cleavage of structural proteins during the assembly of the head of bacteriophage T4. Nature 227:680–685.

Laudet V, Stehelin D, Clevers H. 1993. Ancestry and diversity of the HMG box superfamily. Nucleic Acids Res 21:2493–2501.

Levy O, Dubinsky Z, Achituv Y. 2003. Photobehavior of stony corals: Responses to light spectra and intensity. J Exp Biol 206:4041–4049.

Levy O, Appelbaum L, Leggat W, Gothlif Y, Hayward DC, Miller DJ, Hoegh-Guldberg O. 2007. Light-responsive cryptochromes from a simple

multicellular animal, the coral *Acropora millepora*. Science 318:467–470.

Leys SP, Mackie GO. 1997. Electrical recording from a glass sponge. Nature 387:29–31.

Leys SP, Cronin TW, Degnan BM, Marshall JN. 2002. Spectral sensitivity in a sponge larva. J Comp Physiol [A] 188:199–202.

Liu L, Im H, Cegielski M, LeMagueres P, Schultz W, Krause K, Hastings JW. 2003. Characterization and crystallization of active domains of a novel luciferase from a marine dinoflagellate. Acta Crystallogr D Biol Crystallogr 59:761–764.

Livak KJ, Schmittgen TD. 2001. Analysis of relative gene expression data using real-time quantitative PCR and the $2^{-\Delta\ \Delta CT}$ method. Methods 25:402–408.

Lowenstam HA, Weiner S. 1989. On biomineralization. Oxford: Oxford University Press.

Maldonado M. 2006. The ecology of the sponge larva. Can J Zool 84:175–194.

Mansukhani A, Ambrosetti D, Holmes G, Cornivelli L, Basilico C. 2005. Sox2 induction by FGF and FGFR2 activating mutations inhibits Wnt signaling and osteoblast differentiation. J Cell Biol 168:1065–1076.

Müller WEG. 2006. The stem cell concept in sponges (Porifera): Metazoan traits. Semin Cell Dev Biol 17:481–491.

Müller WEG, Krasko A, Skorokhod A, Bünz C, Grebenjuk VA, Steffen R, Batel R, Schröder HC. 2002. Histocompatibility reaction in tissue and cells of the marine sponge *Suberites domuncula in vitro* and *in vivo*: Central role of the allograft inflammatory factor 1. Immunogenetics 54:48–58.

Müller WEG, Rothenberger M, Boreiko A, Tremel W, Reiber A, Schröder HC. 2005. Formation of siliceous spicules in the marine demosponge *Suberites domuncula*. Cell Tissue Res 321:285–297.

Müller WEG, Wendt K, Geppert C, Wiens M, Reiber A, Schröder HC. 2006. Novel photoreception system in sponges? Unique transmission properties of the stalk spicules from the hexactinellid *Hyalonema sieboldi*. Biosens Bioelectron 21:1149–1155.

Müller WEG, Jochum K, Stoll B, Wang XH. 2008. Formation of giant spicule from quartz glass by the deep sea sponge Monorhaphis. Chem Mater 20:4703–4711.

Müller WEG, Kasueske M, Wang XH, Schröder HC, Wang Y, Pisignano D, Wiens M. 2009. Luciferase a light source for the silica-based optical waveguides (spicules) in the demosponge *Suberites domuncula*. Cell Mol Life Sci 66:537–552.

Müller WEG, Wang X, Schröder HC, Korzhev M, Grebenjuk VA, Markl JS, Jochum KP, Pisignano D, Wiens M. 2010. A cryptochrome-based photosensory system in the siliceous sponge *Suberites domuncula* (Demospongiae). FEBS J 277:1182–1201.

Nickel M. 2006. Like a 'rolling stone': Quantitative analysis of the body movement and skeletal dynamics of the sponge *Tethya wilhelma*. J Exp Biol 209:2839–2846.

Pavans de Ceccatty M. 1989. Les éponges, à l'aube des communications cellulaires. Pour la Sci 142:64–72.

Pfaffl MW. 2001. A new mathematical model for relative quantification in real-time RT-PCR. Nucleic Acids Res 29:2002–2007.

Prosser CL, Nagai T, Nystrom RA. 1962. Oscular contractions in sponges. Comp Biochem Physiol 6:69–70.

Renard E, Vacelet J, Gazave E, Lapébie P, Borchiellini C, Ereskovsky AV. 2009. Origin of the neuro-sensory system: New and expected insights from sponges. Integr Zool 4:294–308.

Ridley SO, Dendy A. 1887. Report on the Monaxonida collected by H.M.S. 'Challenger'. Report on the Scientific Results of the Voyage of the H.M.S. Challenger During the Years 1873–76. Vol. 20. London: *Eyre & Spottiswoode*.

Sachs L. 1984. Angewandte statistik. Berlin: Springer. p 242.

Schröder HC, Sudek S, De Caro S, De Rosa S, Perović S, Steffen R, Müller IM, Müller WEG. 2002. Synthesis of the neurotoxin quinolinic acid in apoptotic tissue from *Suberites domuncula*: Cell biological, molecular biological and chemical analyses. Mar Biotechnol 4:546–558.

Shimomura O. 1980. Presence of coelenterazine in non-bioluminescent marine organisms. Comp Biochem Physiol B Biochem Mol Biol 86:361–363.

Soullier S, Jay P, Poulat F, Vanacker J, Berta P, Laudet V. 1999. Diversification pattern of the HMG and SOX family members during evolution. J Mol Evol 48:517–527.

Steiner M, Mehl D, Reitner J, Erdtmann BD. 1993. Oldest entirely preserved sponges and other fossils from the Lowermost Cambrian and a new facies reconstruction of the Yangtze Platform (China). Berliner Geowiss Abh (E) 9:293–329.

Stevanovic M. 2003. Modulation of SOX2 and SOX3 gene expression during differentiation of human neuronal precursor cell line NTERA2. Mol Biol Rep 30:127–132.

Streit A, Stern CD. 1999. Establishment and maintenance of the border of the neural plate in the chick: Involvement of FGF and BMP activity. Mech Dev 82:51–66.

Thompson JD, Higgins DG, Gibson TJ. 1994. CLUSTAL W: Improving the sensitivity of progressive multiple sequence alignment through sequence weighting, positions-specific gap penalties and weight matrix choice. Nucleic Acids Res 22:4673–4680.

Velarde E, Haque R, Iuvone PM, Azpeleta C, Alonso-Gómez AL, Delgado MJ. 2009. Circadian clock genes of goldfish, *Carassius auratus*: cDNA cloning and rhythmic expression of *Period* and *Cryptochrome* transcripts in retina, liver, and gut. J Biol Rhythms 24:104–113.

Wang XH, Hu S, Gan L, Wiens M, Müller WEG. 2010. Sponges (Porifera) as living metazoan witnesses from the Neoproterozoic: Biomineralization and the concept of their evolutionary success. Terra Nova 22:1–11.

Wegner M. 1999. From head to toes: The multiple facets of SOX proteins. Nucleic Acids Res 27:1409–1420.

Wiens M, Koziol C, Hassanein HMA, Batel R, Müller WEG. 1998. Induction of gene expression of the chaperones 14-3-3 and HSP70 induced by PCB 118 (2,3́,4,4́,5-pentachlorobiphenyl) in the marine sponge *Geodia cydonium*: Novel biomarkers for polychlorinated biphenyls. Mar Ecol Prog Ser 165:247–257.

Wiens M, Batel R, Korzhev M, Müller WEG. 2003. Retinoid X receptor and retinoic acid response in the marine sponge *Suberites domuncula*. J Exp Biol 206:3261–3271.